



1 **Technical note: Validation of Aleppo pine transpiration rate**
2 **measurements using the heat ratio method under laboratory conditions**

3 Ana M. Sabater^{1,2}, José Antonio Valiente³, Juan Bellot^{2,4}, Alberto Vilagrosa^{1,2}.

4 ¹Mediterranean Centre for Environmental Studies (Fundación CEAM), Joint Research
5 Unit University of Alicante–CEAM, PO Box 99, C. San Vicente del Raspeig, s/n,03080
6 Alicante, Spain.

7
8 ²Department of Ecology, University of Alicante, C. San Vicente del Raspeig, s/n, 03080
9 Alicante, Spain.

10 ³Mediterranean Centre for Environmental Studies (Fundación CEAM), C. Charles R.
11 Darwin 14, Parque Tecnológico, 46980 Paterna, Valencia, Spain.

12 ⁴The Multidisciplinary Institute for Environmental Studies (IMEM), University
13 of Alicante, C. San Vicente del Raspeig, s/n, 03080 Alicante, Spain.

14 *Correspondence to:* Ana M. Sabater (sabaterblasco@gmail.com)

15 **Abstract**

16 Tree transpiration considerably contributes to evaporative fluxes to the atmosphere in
17 terrestrial ecosystems. Accurate transpiration quantification promotes the knowledge of
18 water consumption by forests and could favour an adaptive forest management, especially
19 in a global change context. Tree transpiration can be measured by a wide range of
20 methods, and one of the valued ones is sap flow measurements. However, species-specific
21 validations of techniques are required. Hence the objectives of this study were to validate
22 transpiration rate measurements by the heat ratio method (HRM) in juvenile Aleppo pine
23 trees (*Pinus halepensis* Mill.) by using the probe misalignment correction proposed by
24 Larsen et al. (2020). This study simultaneously recorded the transpiration rate by tree sap
25 flow following the HRM technique (T_{HRM}) and tree water losses by load cells (T_{OBS}).
26 These measurements were taken in combination with the environmental variables that
27 control this process such as different vapour pressure deficit (VPD) ranges of air and the
28 soil relative extractable water (REW). The results showed an accurate linear
29 correspondence between T_{OBS} and the transpiration rate measurements both without and
30 with probe misalignment correction, T_{HRM} and $T_{HRM MIS}$, respectively, but interestingly
31 underestimations at high transpiration rates were observed. However, underestimations
32 were removed when applying probe misalignment correction. $T_{HRM MIS}$ showed a good



33 relation between the VPD_xREW interaction. This study supports the notion that HRM
34 offers accurate low values under a wide range of abiotic conditions, and is useful in
35 isohydric species with low transpiration rates like Aleppo pine. To conclude, our results
36 support the validation of both transpiration rate measurements by the T_{HRM} and probe
37 misalignment correction in Aleppo pine under different environmental laboratory
38 conditions.

39 **1. Introduction**

40 Global change scenarios not only predict increasing temperature and changes in
41 precipitation patterns, but also higher drought intensity and longer duration (IPCC, 2021).
42 Climate alterations will affect ecosystems' function and survival by promoting changes
43 in plant water use (Lindner et al. 2010). Quantifying soil-vegetation-atmosphere water
44 fluxes is critical for understanding both current and future ecosystem hydrology, and for
45 providing adaptive forest management. In forest ecohydrology, transpiration is the main
46 actual terrestrial evapotranspiration (ET_a) component (Jasechko et al. 2013). On average,
47 worldwide forests' transpiration fraction represents 64% of the total ET_a water fluxes to
48 the atmosphere (Good et al. 2015). In Mediterranean Aleppo pine forests, transpiration
49 can contribute to 50 % ET_a in an annual budget (Sabater et al. 2021). Additionally,
50 transpiration provides plant-level information and is important in water status, leaf
51 cooling and nutrient transport.

52 Tree or plant transpiration can be measured by a wide range of methods, such as
53 lysimeters (Swanson and Whitfield, 1981; Ruiz-Yanetti et al. 2016), isotopic approaches
54 (Scheidegger et al. 2000), atmospheric techniques (e.g. eddy covariance; Williams et al.
55 2004), models (Fernandes et al. 2015; Sperry et al. 2019) and sap flow measurements
56 (Smith and Allen, 1996; del Campo et al. 2014). Sap flow methods have been used since
57 the start of the 20th century by tracing water movement through xylem tissues (Huber,
58 1928). The sap flow technique is often used in woody species at the whole plant level
59 because it presents several advantages by allowing, for example, continuous readings, it
60 is not limited to single or a few leaf measurements, and it can be applied irrespectively of
61 both orographic and atmospheric conditions (Forster, 2017). Of the several methods
62 available to estimate sap flow, the most popular ones are thermal dissipation, heat pulse
63 velocity and heat field deformation.



64 The heat ratio method (HRM) has been used in many articles (Vandegehuchte and Steppe,
65 2012) and is quite reliable for determining transpiration (Fernández et al. 2001; Williams
66 et al. 2004). The HRM offers excellent advantages, such as: applications in the diameters
67 of tree trunks above 25 cm (Swanson, 1994); the detection of low and reverse flows due
68 to a rapid thermal response (Burgess et al. 2001; Marshall, 1958). The heat pulse in the
69 HRM is discrete, unlike other techniques that use constant pulses. Due to rapid pulse
70 diffusion when conduction and convection effects are comparable to one another,
71 temperature rises at a point and reaches its maximum value before the centre of the heat
72 pulse goes up to that point (Marshall, 1958).

73 However, the HRM presents several calculation steps to convert the measurements of
74 temperatures before and after the heat pulse into sap flow measurements, which are
75 associated with different uncertainties that can modify the accuracy of measurements
76 (Looker et al. 2016). One of the main sources of uncertainty is the spacing of HRM probes
77 in trunks. Larsen et al. (2020) proposed probe misalignment correction in Aleppo pine
78 trunks. This approach proposes a methodology that estimates minor changes in the
79 resulting spacing of probes compared to the theoretically prescribed one. This correction
80 can also detect the evolution of these corrections over time by compiling the effect of
81 growth or physiological evolution on probe positions. Applying Larsen's corrections can
82 provide accuracy transpiration quantification and also reduce costs because probes do not
83 need to be frequently replaced. Even though sap flow measurements are reasonably
84 corrected when applying probe misalignment correction, the above-cited research work
85 did not provide a validation of measurements.

86 Several works describe the importance of quantitative calibrations in sap flow methods
87 for both commercial and lab-built probes to guarantee the highest quality sap flow
88 measurements (Dix and Aubrey, 2021). In the scientific disciplines (e.g., ecohydrology)
89 that require many probes, the cost of commercial probes can be the main disadvantage
90 (Wiedemann et al. 2016). HRM lab-built probes can be adapted to specific plant
91 characteristics. They are also affordable compared to commercial ones because several
92 probes are needed for accurate monitoring and to replicate a study area (Davis et al. 2012).
93 HRM lab-built probes have been used to measure Aleppo pine sap flow in technical works
94 (Davis et al. 2012; Larsen et al. 2020). Davis et al. (2012) describe a guide for lab-built
95 probes and provide accurate results in qualitative HRM calibration.



96 Aleppo pine (*Pinus halepensis* Mill.) is one of the most representative and extensive
97 forest species in Mediterranean forests and covers around 25,000 km² (Quézel, 2000).
98 Compared to other Mediterranean species (e.g. *Quercus* sp.), Aleppo pine presents an
99 isohydric strategy with a water-saver response and shows low transpiration rates (Vicente
100 et al. 2018). Drivers of Aleppo pine transpiration vary among climatic contexts, and
101 relative extractable water (REW) and vapour pressure deficit (VPD) are the most
102 important ones (Chirino et al. 2015; Larsen 2021). Accurate Aleppo pine transpiration
103 measurements and their drivers are needed to understand the integration of soil-plant-
104 atmosphere water fluxes and to, hence, plan hydrological and climatological studies and
105 forest ecosystem research.

106 Due to large covered areas and the relevance of this species, Aleppo pine transpiration
107 quantifications are key for the ecohydrology knowledge in the Mediterranean Basin and
108 its forest management. This study tries to offer a response to the need to perform
109 calibration on sap flow probes in an isohydric water-saver species (i.e. low transpiration
110 rates) by providing high-quality sap flow data (Dix and Aubrey, 2021). This study aims
111 to: i) validate the Aleppo pine transpiration rates measured by the HRM technique under
112 different laboratory environmental conditions compared to load cells as a direct method
113 to measure the plant transpiration rate; ii) test the probe misalignment correction proposed
114 by Larsen et al. (2020) under different environmental conditions. An auxiliary objective
115 is to assess the environmental drivers of Aleppo pine transpiration under laboratory
116 conditions. Aleppo pines were submitted to different environmental conditions, such as
117 VPD and REW, as drivers of transpiration oscillations and transpiration rates, determined
118 by two different techniques HRM and load cells. The hypotheses were: i) the high
119 transpiration values measured by the HRM technique globally underestimated high sap
120 flow rates specifically, while low sap flow rates were measured with higher accuracy due
121 to the rapid thermal response of the HRM method; ii) transpiration in a wide range of
122 values measured by the HRM technique and corrected through the methodology proposed
123 in Larsen et al. (2020) presented higher accuracy measurements and smaller bias errors
124 than without probe misalignment correction; iii) VPD and REW conditioned transpiration
125 by promoting stomatal closure under high evaporative demand and/or water scarcity
126 conditions. However, the interaction of the two variables was expected to be the main
127 factor in Aleppo pine transpiration.

128



129 **2. Material and methods**

130 **2.1. Plant material**

131 The experiment was conducted in the Plant Experimentation Unit of the University of
132 Alicante (Spain) over 57 days in spring 2019. Three juvenile Aleppo pine individuals
133 were used for this experiment. Individuals were grown in pots filled with mixed substrate
134 with peat, compost and coconut fibre. Soil volume was measured as the geometric volume
135 delimited by each pot. For the soil apparent density measurements, the weight and volume
136 of soil samples were calculated under saturated conditions. Then soil sample were dried
137 for three days at 60 °C. The resulting dry weights were divided by the initial volume to
138 obtain soil apparent density. After the experiment, the three pines were cut and separated
139 into leaves and woody components (trunk and branches), which were weighed directly
140 after cutting to obtain the fresh individual weight. Then they were dried for seven days at
141 60 °C and were finally weighed to obtain the dry weight. Sap wood water content (m_c)
142 was measured following Eq. (1), where w_f and w_d were the fresh and oven-dried weight
143 of the trunks sample, respectively (Marshall, 1958).

144
$$m_c = \frac{(w_f - w_d)}{w_d} \quad (1)$$

145 Basic wood density (p_b) was measured as the dry weight divided by the green volume
146 (Marshall, 1958). The green volume was measured by the water displacement of four
147 wooden cubes per tree (approx. 20x20x20 mm). Cubes were dried for seven days at 60
148 °C and weighed to obtain dry weight measurements. The sap wood area was measured as
149 the area occupied by exudates of water and sap after cutting the trunk at the breast height.
150 Before the experiment, a calibration analysis between the known weights and the weight
151 measured by load cells was performed to test and adjust linearity in the load cells (Table
152 1).

153 **2.2. Experimental setup**

154 Aleppo pine transpiration was measured using two simultaneous, but different and
155 independent, techniques: the heat ratio method by means of sap flow probes (T_{HRM}) and
156 the weighing of water losses by means of load cells (lysimeter technique, T_{OBS}). Sap flow
157 and water losses were two different approximations followed to estimate the transpiration
158 rate per tree (T , kg h^{-1}). Pots were wrapped in film and plastic bags to avoid evaporation
159 loss directly from soil. The pine individuals were located in the Plant Experimentation
160 Unit a week before the experiment started for them to acclimatise to the experimental



161 conditions. The limitation of having only three individuals was overcome by including a
162 long experimental period (57 days) using half-hourly measurements.

163 **2.3. Heat ratio method**

164 The heat ratio method (HRM) is described in detail in Burgess et al. (2001), and the
165 principle of measurements is found in Williams et al. (2004). The HRM employs
166 temperature probes inserted into the active xylem at equal distances (0.6 cm) down- and
167 upstream from the heat probe. More details of the lab-built construction of the HRM
168 probes are found in Sect. Appendix A and Appendix B.

169 For a given tree, sap velocity (V , cm h^{-1}) was obtained following Eq. (2), (6) and (7)
170 described in Burgess et al. (2001). Then the transpiration rate (T_{HRM} , kg h^{-1}) was upscaled
171 by multiplying each sap wood area per tree (Table 1).

172 Transpiration was also improved by applying the probe misalignment correction
173 described in Larsen et al. (2020) ($T_{\text{HRM MIS}}$, kg h^{-1}). In this case, Eq. (2) in Burgess et al.
174 (2001) was not applied. Instead, a modification of Eq. (8) described in Larsen et al. (2020)
175 was applied to calculate two different sap velocities: V_1 and V_2 . For V_1 calculations it was
176 assumed that the distance between the heat and the downstream temperature probe (X_1)
177 underwent misalignment (different to 0.6 cm), while the distance between the heater and
178 upstream probe (X_2) was fixed to -0.6 cm. The opposite was assumed to calculate the
179 other sap velocity (V_2). To evaluate X_1 and X_2 , it was necessary to achieve zero-flow
180 conditions, which were identified as night episodes when null-weight variations were
181 recorded by the load cells per tree. Four events of zero-flow conditions were selected
182 during the study period. Events were clearly detected at night (23:00-2:30), when the
183 vapour pressure deficit came close to zero. An average of the half-hour temperature
184 readings per event was performed and Eq. (6) in Larsen et al. (2020) was applied. Finally,
185 the average of the resulting X_1 and X_2 values for each of the zero-flow events (Table D1)
186 were used in Eq. (8) in Larsen et al. (2020) to obtain V_1 and V_2 . This means that the
187 resulting value described in Table D1 replaced the slope and intercept described in Eq.
188 (8) in Larsen et al. (2020). Thus, the modification herein applied did not take into account
189 temporary probe misalignment behaviour because no temporal dependence of X_1 and X_2
190 was observed among the selected events. V_1 and V_2 were averaged (\bar{V}). Then \bar{V} was
191 applied to Eq. (8) detailed in Burgess et al., (2001), and it was upscaled to transpiration
192 by multiplying per sap wood area.



193 Table 1. Features associated with each pine individual.

| | Pine number 1 | Pine number 2 | Pine number 3 |
|---|---|---|---|
| Soil volume (m ³) | 0.061 | 0.061 | 0.060 |
| Soil apparent density (g cm ⁻³) | 0.133 | 0.149 | 0.163 |
| Fresh individual weight (kg) | 12.85 | 9.87 | 6.28 |
| Dry individual weight (kg) | 8.8 | 6.4 | 4.2 |
| Percentage of dried-leave weight over the dry individual weight (%) | 18 | 24 | 30 |
| Sap wood water content (m_c , dimensionless) | 0.42 | 0.58 | 0.60 |
| Basic wood density wood (p_b , kg m ⁻³) | 0.50 | 0.53 | 0.49 |
| Sap wood area (cm ²) | 22.05 | 15.55 | 12.86 |
| Absolute error of load cell (g) | 23 | 27 | 58 |
| Load cell model | GRUPO EPELSA, Model MV2, Emax 500 Kg | GRUPO EPELSA, Model MV2, Emax 500 Kg | GRUPO EPELSA, Model LC2, Emax 100 Kg |

194

195

196

197



198 **2.4. Load cells design and environmental measurements**

199 Load cells were sampled on a 10 minute basis. Due to the inherent data scattering found
200 in this output type, a moving average was used over each weight time series. To estimate
201 water losses, the difference between the current and previous averaged weight values was
202 used.

203 Soil water content (SWC) was indirectly calculated using the weighing data recorded by
204 the load cells, soil field capacity and apparent density measured in the laboratory, and by
205 adding each water volume during the irrigation pulses. The following equation was
206 applied to obtain relative extractable water (REW) (Granier, 1987), where SWC_i was the
207 instantaneous value of SWC. SWC_{max} and SWC_{min} were the maximum and minimum
208 values of the data series, respectively.

209
$$REW = \frac{SWC_i - SWC_{min}}{SWC_{max} - SWC_{min}} \quad (2)$$

210 The air vapour pressure deficit of the atmosphere (VPD, kPa) was calculated from the
211 temperature and relative humidity values (Allen et al. 1998).

212 Actual vapour pressure (ea) = $0.6108^{(17.27 \times \text{Temp}) / \text{Temp} + 273.3}$

213 Saturation vapour pressure (es) = $ea \times \frac{RH}{100}$

214 Vapor pressure deficit (VPD) = $es - ea$ (3)

215

216 Air temperature (Temp, °C) and relative humidity (RH, %) were recorded by an EE08-
217 PFT1V11E605/T48 High-Precision Miniature T/H Sensor. Global solar radiation ($W m^{-2}$)
218 was recorded by an Apogee Instruments Ltd. SP-110-C: Self-Powered Pyranometer
219 Sensor.

220 All records were recorded by a datalogger (Campbell Scientific CR800 Series
221 Datalogger) associated with a multiplexor (Campbell Sci model AM16/32B Relay
222 Analogue Multiplexer) and connected to a 12 V battery (Lead Acid Battery, RS Pro, 12
223 V 55 Ah, AGM). All the variables were measured on a 10-minute basis, except for T_{HRM} ,
224 whose resolution was half-hourly.

225

226

227



228 2.5. Data analysis

229 The obtained T_{OBS} and T_{HRM} data did not follow normal distributions, but strongly skewed
230 distributions towards values below 0.02 kg h^{-1} . Two data filters were used to achieve
231 normal distributions to then perform coherent statistical analyses. Firstly, a radiation filter
232 threshold was defined as 5 W m^{-2} to select only the data corresponding to the diurnal
233 conditions. Secondly, random selection was employed to attain enough data values at
234 different bins that defined normal distribution. To validate the heat ratio transpiration
235 measurements, a linear model was fitted in R (R Core Team 2021) by taking T_{OBS} as the
236 dependent variable, and T_{HRM} and $T_{HRM MIS}$ as the independent variables. The root mean
237 squares of the models were fitted by the ‘rmse’ function of the hydroGOF R Package
238 (Zambrano-Bigiarini, 2020).

239 To test the environmental drivers of $T_{HRM MIS}$ under laboratory conditions, a linear mixed-
240 effects model (nlme package) was fitted in R (R Core Team 2021) with $T_{HRM MIS}$ as the
241 dependent variable, VPD, REW and their interaction (VPD \times REW) as the fixed effects
242 factors, and Aleppo pine individuals were fitted as a random effect. Both VPD and REW
243 were the continuous variables. Global solar radiation was not included because it
244 correlated highly with VPD (cor.test > 0.8). Marginal and conditional R^2 were calculated
245 using the piecewiseSEM R package (Lefcheck, 2016) to assess the proportion of variance
246 explained by the fixed and by both the fixed and random effects (Nakagawa and
247 Schielzeth, 2013).

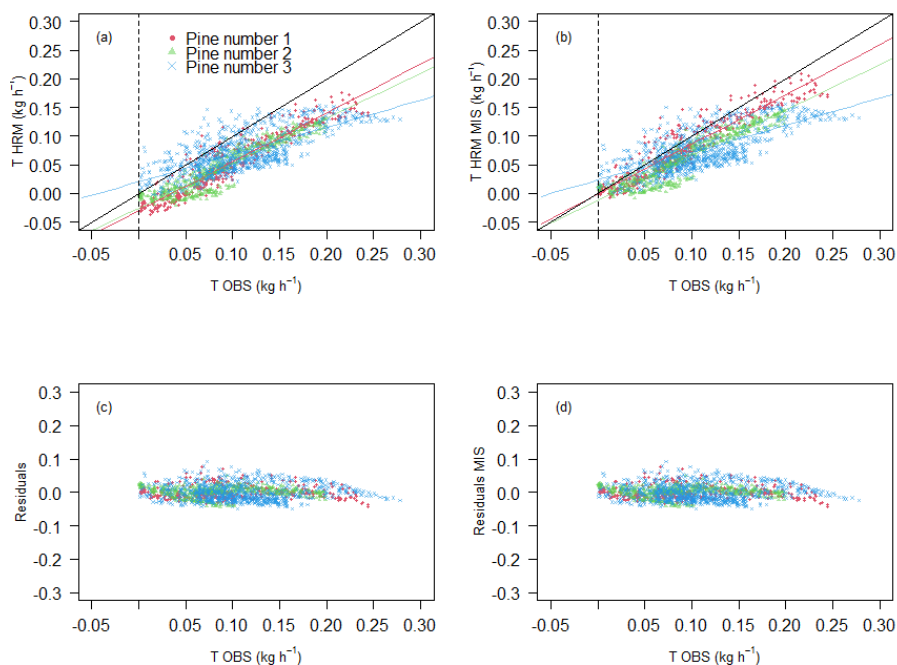
248 3. Results

249 3.1. Comparison of the transpiration rate using the heat ratio method technique and 250 load cells

251 The coefficients of determination showed a linear relation between the transpiration
252 measured by T_{HRM} and load cells, T_{OBS} (Fig. 1a and 1c), with good prediction ability ($R^2 >$
253 0.5; Table 2). The linear relations showed slopes lower than 1, which imply an
254 underestimation in the absolute values (Fig. 1a). However, accuracy was high at low rates,
255 but accuracy was low and provided transpiration underestimations at high rates (Fig. 1a,
256 Fig. D1a, c, e). The biggest difference between the method measurements ($T_{OBS} - T_{HRM}$ or
257 absolute error) that represented the greatest underestimations were 0.11 kg h^{-1} , 0.09 kg h^{-1}
258 ¹ and 0.15 kg h^{-1} for pine number 1, pine number 2 and pine number 3, respectively (Fig.
259 D1a, c, e). The T_{HRM} values around zero were different among pine individuals, even



260 though they presented negative values, especially in pine number 1 (Fig. 1a).



261

262 Figure 1. (a) Linear regression of the transpiration rates measured by load cells (T_{OBS}) vs.
 263 those measured by heat ratio method probes (T_{HRM}). (b) Linear regression of T_{OBS} vs.
 264 T_{HRM} rectified by the probe misalignment correction proposed in Larsen et al. (2020)
 265 ($T_{HRM MIS}$). (c) Residuals of the models (Table 2) vs. T_{OBS} . (d) Residuals of the models
 266 using misalignment correction data (Table 3) vs. T_{OBS} . The black line shows the curve
 267 defined by the 1:1 simulated regression. The dashed line depicts the 0 kg h^{-1} T_{OBS} values.

268 Table 2. Summary statistics of the linear model of the transpiration rate measured by the
 269 heat ratio method probes (T_{HRM} , kg h^{-1}) according to the transpiration rate measured by
 270 load cells (T_{OBS} , kg h^{-1}).

| | Pine number 1 | Pine number 2 | Pine number 3 |
|-----------|--------------------|--------------------|-------------------|
| Intercept | -0.030 ± 0.002 | -0.026 ± 0.002 | 0.020 ± 0.002 |
| T_{OBS} | 0.853 ± 0.016 | 0.785 ± 0.014 | 0.475 ± 0.017 |
| R^2 | 0.88 | 0.86 | 0.50 |
| p-value | $< 2.2e-16$ | $< 2.2e-16$ | $< 2.2e-16$ |

271



272 When the probe misalignment correction proposed by Larsen et al. (2020) was applied
273 ($T_{HRM\ MIS}$), the ability of the regressed model prediction was also high (Fig. 1b and 1d,
274 Table 3). The slope and intercept between $T_{HRM\ MIS}$ and T_{OBS} came closer to 1 and 0,
275 respectively (Table 3), which promoted high accuracy along transpiration rates. $T_{HRM\ MIS}$
276 presented lower root mean squares values than the T_{HRM} models, which means more
277 accurate measurements when probe misalignment correction was applied (Table 4a and
278 4b). There were fewer negative $T_{HRM\ MIS}$ values than negative T_{HRM} values, and the
279 transpiration *versus* T_{OBS} relations were much more homogenous between pines for the
280 particular case of the misalignment correction technique than for the method without
281 correction (Fig. 1a and Fig. 1b). Pine number 1 presented the highest probe misalignment
282 value, while pine number 3 had the lowest (Table D1). Likewise, the highest and lowest
283 root mean squares values were for pine number 1 and pine number 3, respectively (Table
284 4b). Despite the fact that pine number 3 obtained the lowest misalignment value, it also
285 had the least accurate load cell, with absolute errors above double that for the other load
286 cells (Table 1). This fact was taken as a less accurate comparative result than in the other
287 pines.

288 The distribution of residuals when a regression analysis based on T_{OBS} was performed
289 was constant along T_{HRM} and $T_{HRM\ MIS}$ (Fig. 1c and 1d). The maximum underestimations
290 ($T_{OBS} - T_{HRM\ MIS}$) per individual were 0.08 kg h^{-1} , 0.08 kg h^{-1} and 0.15 kg h^{-1} for pine
291 number 1, pine number 2 and pine number 3, respectively (Fig. A3b, d, f).

292 Table 3. Summary statistics of the linear model of transpiration rates measured by the
293 heat ratio method probes corrected by the probe misalignment correction proposed by
294 Larsen et al. (2020) ($T_{HRM\ MIS}$, kg h^{-1}) according to the transpiration rate measured by load
295 cells (T_{OBS} , kg h^{-1}).

| | Pine number 1 | Pine number 2 | Pine number 3 |
|----------------|--------------------|--------------------|-------------------|
| Intercept | -0.002 ± 0.002 | -0.012 ± 0.001 | 0.023 ± 0.002 |
| $T_{HRM\ OBS}$ | 0.871 ± 0.017 | 0.790 ± 0.014 | 0.476 ± 0.017 |
| R^2 | 0.88 | 0.87 | 0.50 |
| p-value | $< 2.2e-16$ | $< 2.2e-16$ | $< 2.2e-16$ |

296

297

298



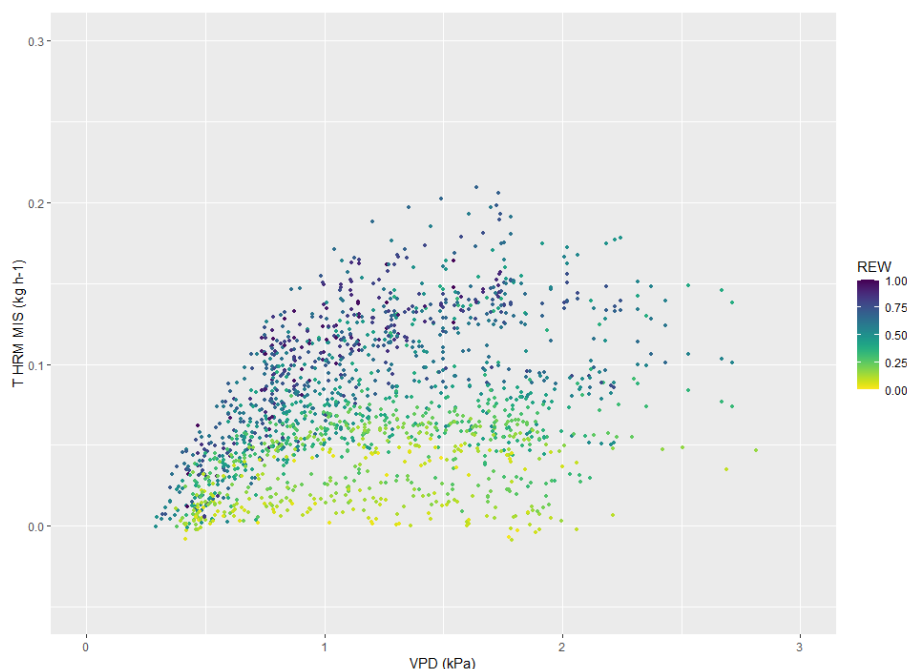
299 Table 4. Root mean square of the regression residuals and differences between the
300 transpiration values determined by the different methods: load cells (T_{OBS}) and the heat
301 ratio method (T_{HRM} and $T_{HRM MIS}$). Lower root mean squares values represent a more
302 accurate relation between the variables T_{HRM} vs. T_{OBS} and $T_{HRM MIS}$ vs. T_{OBS} . Letters are
303 associated with the panels in Fig. 1.

| | Pine number 1 | Pine number 2 | Pine number 3 |
|-----------------------------------|---------------|---------------|---------------|
| (a) T_{HRM} vs. T_{OBS} | 0.049 | 0.049 | 0.053 |
| (b) $T_{HRM MIS}$ vs. T_{OBS} | 0.025 | 0.037 | 0.051 |
| (c) Residuals vs. T_{OBS} | 0.11 | 0.10 | 0.13 |
| (d) Residuals MIS vs. T_{OBS} | 0.11 | 0.10 | 0.13 |

304

305 3.2 Effect of environmental conditions on the transpiration response

306 The half-hourly REWs ranged from 0 to 1 (dimensionless), while the hourly VPD attained
307 minimum and maximum values of 0.27 kPa and 2.82 kPa, respectively. The $T_{HRM MIS}$
308 values ranged from -0.01 ± 0.01 kg h⁻¹ to 0.17 ± 0.01 kg h⁻¹ (Fig. 2). Model predictors
309 included a positive interaction between VPD and REW. The model showed good
310 predictive ability for the environmental conditions (R^2 marginal of 0.61; Table 5). Model
311 predictors included a positive interaction between VPD and REW (Table 5). Global solar
312 radiation was not included because it correlated highly to VPD (cor.test > 0.8). The
313 VPDxREW interaction resulted in simple patterns in the variation of both $T_{HRM MIS}$.
314 Higher $T_{HRM MIS}$ values were predicted under the conditions according to both the high
315 REW and high VPD values (Fig. 2).



316

317 Figure 2. Representation of the response of the transpiration rate measured by the heat
 318 ratio method probes corrected by Larsen's misalignment probes corrections ($T_{HRM MIS}$) to
 319 the environmental variables interaction ($VPD \times REW$, vapour pressure deficit x relative
 320 extractable water). REW was represented as a gradient scale colour, where purple depicts
 321 wet conditions and yellow dry conditions. The figure is a graphical explanation of the
 322 models in Table 5.

323 Table 5. Summary statistics of the linear mixed-effects models of the transpiration
 324 measured by heat ratio method (T_{HRM}) according to the environmental variables. Pine
 325 individuals are fitted as a random factor. Abbreviations: VPD: vapour pressure deficit,
 326 REW: relative extractable water. The cross indicates the $VPD \times REW$ interaction. Asterisk
 327 (*) depicts a p-value lower than 0.05.

| $T_{HRM MIS}$ | Fixed effects | Random effects (pine individuals) |
|-------------------|----------------------|--------------------------------------|
| Residual error | - | 0.014 |
| Intercept | $0.023 \pm 0.009^*$ | 0.025 |
| VPD | $-0.006 \pm 0.003^*$ | |
| REW | $0.014 \pm 0.007^*$ | |
| $VPD \times REW$ | $0.094 \pm 0.005^*$ | |
| R^2 Marginal | 0.61 | |
| R^2 Conditional | 0.70 | |



328 4. Discussion

329 A good linear relation appeared between the transpiration rate measurements by
330 following the HRM technique (T_{HRM} and $T_{HRM MIS}$, with and without probe misalignment
331 correction, respectively) and load cells (T_{OBS}). At a transpiration rate lower than 0.10 kg
332 h^{-1} , the transpiration measurements showed the highest accuracy, which agrees with the
333 theory of the heat ratio method (HRM), having a rapid thermal response time (Burgess et
334 al. 2001; Burgess and Dawson, 2008). Therefore, our results support the usefulness of the
335 HRM in Aleppo pine transpiration rates because this method is capable of acquiring
336 accurate data when this species drastically reduces transpiration under Mediterranean
337 summer conditions. For other species, this method has been reported as useful for
338 measurements taken under night conditions (Forster, 2017). Interestingly, the
339 measurements in this study showed qualitatively lower accuracy at transpiration rates
340 above 0.10 kg h^{-1} . This fact has also been reported in previous reviews (Burgess and
341 Dawson, 2008) in commercial methods (Fuch et al. 2017) and in the method validation
342 for other species (Bleby et al. 2004). However, heat pulse methods present lower
343 underestimations across sap flow methods (Steppe et al. 2010).

344 The results herein obtained support the validation of the HRM in Aleppo pine. A sporadic
345 temperature ratio measurement must be converted into a complete tree transpiration rate
346 by a few equations that combine wood- and tree-specific parameters. For this reason, the
347 accuracy of transpiration rates can be explained by the experimental individual-specific
348 measurements of the variables involved in transformations: sap wood water content (m_c),
349 basic wood density (p_b) and sap wood area. Some reports about transpiration estimations
350 in *Pinus* sp. using the HRM technique apply the same value for m_c and p_b for all the
351 individuals (del Campo et al. 2014; Larsen et al. 2020), while other articles apply different
352 values per individual (Alvarado-Barrientos et al. 2013; Eliades et al. 2018). In this study,
353 individual-specific measurements were obtained and applied as transpiration rate
354 conversions. Contrary, if the mean value of the three individuals for m_c and p_b had been
355 applied, the resulting maximum underestimations ($T_{OBS} - T_{HRM}$) would have increased,
356 with values of 0.25 kg h^{-1} , 0.20 kg h^{-1} and 0.30 kg h^{-1} for pine number 1, pine number 2
357 and pine number 3, respectively.

358 Some reports describe uncertainties in transpiration measurements associated with sap
359 wood area (Hatton et al. 1992), with m_c (López-Bernal et al. 2014; Vandegehuchte and



360 Steppe 2012; Vergeynst et al. 2014), and also with both m_c and p_b (Swanson, 1983), and
361 their relationship with thermal diffusivity (Looker et al. 2016). Contrarily to the thermal
362 diffusivity measurements based on m_c and p_b (Burgess et al. 2001; Vandegehuchte and
363 Steppe 2012), the thermal diffusivity originally noted by Marshall (1958) was herein
364 applied ($2.5 \times 10^{-3} \text{ cm}^2 \text{ s}^{-1}$). This value is an intermediate between the thermal diffusivity
365 of water and dry wood ($1.4 \times 10^{-3} \text{ cm}^2 \text{ s}^{-1}$ and $4.0 \times 10^{-3} \text{ cm}^2 \text{ s}^{-1}$, respectively). Similar
366 thermal diffusivity values appear in angiosperm when applying Burgess et al. (2001)
367 measurements. This scenario suggests that employing the thermal diffusivity proposed by
368 Marshall (1958) does not imply major errors in transpiration measurements.

369 Once probes are inserted into trunks, it is difficult to assess how accurate probe alignment
370 is. To gain maximum accuracy, the validation of the probe misalignment correction
371 introduced by Larsen et al. (2020) as a modification of the former proposed by Burgess
372 et al. (2001) presents the highest accuracy compared with the HRM technique without
373 correction. Probe misalignment correction Larsen et al. (2020) not only provides higher
374 transpiration rate quantification accuracy, but also shifts negative or approximately zero
375 transpiration rates among other values. Due to the water-saver Aleppo pine strategy, the
376 accuracy of the low transpiration rates of this technique ensures good transpiration rate
377 measurements under high evaporative demand and water scarcity conditions. When
378 applying correction, the underestimation at flows above 0.10 kg h^{-1} decreased, which led
379 to higher accuracy in the transpiration rate estimations under wetter and colder conditions.
380 Consequently, the improvement made while taking transpiration rate measurements when
381 applying correction promoted better estimations along the seasonal variability of
382 Mediterranean areas. However, magnitude varied depending on the degree of probe
383 misalignment. The error variability in the magnitude of the transpiration rate has been
384 shown in previous reports (Sun et al. 2012; Rubilar et al. 2017). The larger the probe
385 misalignment, the greater the correction of the T_{HRM} values, and the smaller the probe
386 misalignment, the lesser the correction of T_{HRM} values. For this reason, the results in this
387 paper support the application of probe misalignment correction in all the sampled
388 individuals.

389 Despite not only the main focus of this study being the validation of the HRM technique
390 for water-saver isohydric species with low transpiration rates, but also probe
391 misalignment correction in this technique, it is interesting to report that the VPDxREW
392 interaction was the main environmental driver of Aleppo pine transpiration under



393 laboratory conditions. The importance of VPD and REW in evaporative fluxes has been
394 shown separately in several articles about Mediterranean vegetation (Chirino et al. 2011;
395 Manrique et. al 2017). However, very few reports are available about the interaction
396 between VPD and soil water content (Grossiord et al. 2020). Aleppo pine is extensive in
397 Mediterranean regions which, according to climate change projections, are one of the
398 world regions where air temperature and extreme drought are expected to increase, and
399 precipitation patterns are predicted to change (Lionello and Scarascia, 2018). These
400 predictions will directly increase VPD and modify REW, which may have impacts on
401 vegetation. In fact, a rising temperature and changes in precipitation regimes have already
402 been related to dieback and forest decay processes worldwide (Allen et al. 2015;
403 Hartmann et al. 2018). Future research should investigate if the same interaction occurs
404 under field conditions compared to those studies that have shown simpler drivers.

405 In relation to technical issues, the cost of plant material, time and equipment is high in
406 calibration experiments, and frequently it is a limiting factor. Besides, transport logistics
407 and performing calibration with increasing tree size are challenges (Dix and Aubrey,
408 2021). In this study, plant material only contained three juvenile Aleppo pine individuals
409 and the equipment for measuring water losses contained two types of load cells with
410 distinct resolutions. Nevertheless, the confidence in the results herein presented is
411 strengthened by the large temporal scale and the wide range of environmental conditions.
412 The ranges of environmental conditions (VPD and REW) used in this paper is consistent
413 with the range observed in fieldwork studies. Although it is true that similar
414 environmental conditions to those of a Mediterranean summer (high evaporative demand
415 and scarce water availability) were not simulated, under our conditions Aleppo pine
416 induces stomatal closure and transpiration rates drastically drop.

417 **5. Conclusions**

418 It should be noted that the results reported in this paper are associated with Aleppo pine
419 species, which is an isohydric water-saver species with low transpiration rates well
420 adapted to drylands. Thus, the conclusions are related to this functional plant ecological
421 response and a specific method (HRM technique). However, this paper provides not only
422 a validation of transpiration rate measurements following the theory and transformation
423 described in Burgess et al. (2001), but also the first validation of the probe misalignment
424 correction proposed by Larsen et al. (2020). The results highlighted the importance of
425 measuring specific individual physiological properties (m_c , p_b , sap wood area) to reduce



426 errors in transpiration measurements, and suggested corrections to obtain accurate
427 absolute quantifications of transpiration rates in species with a functional plant strategy
428 based on low transpiration rates like those in drylands and Mediterranean areas.

429 **Appendices**

430 **Appendix A. Lab-building of the heat ratio method probes**

431 Heat ratio probes were designed as described by Burgess et al. 2001 and were built
432 following the original design detailed by Davis et al. (2012). The sap wood depth of the
433 Aleppo pine individuals was shallower than the sap wood depth of the aged individuals,
434 which are normally measured in the field (Fig. A2b). Thus, the longitude of the needle
435 and their associated material were halved. The heat ratio method (HRM) requires three
436 probes: a heater and two thermocouples. Thermocouples were constituted by 25 cm
437 constantan (TFCC-005-100) and a type E junction of 25 cm chromium (TFCH-005-100).
438 The constantan (0.3 cm) and chromium wires (2.3 cm) were welded together and placed
439 firstly inside a glass tube (0.1 cm x 2.3 cm, MODEL), and secondly inside a needle (0.13
440 cm x 2.3 cm, STERICAN Hypodermic Needles). The heater was made of a 20 cm
441 constantan wire of (TFCC-005-100) and a 4 cm-long aluminium wire. They were welded
442 together (0.5 cm). The constantan wire was coiled in 2 cm of aluminium wire and was
443 placed inside a needle of 2.3 cm. A combination resistance of 7.9 ohms (TE connectivity,
444 Series ER58, 7 W Axial, $\pm 5\%$: $4.7 \Omega + 2.2 \Omega \pm 1 \Omega$) was added to the ends of the wire to
445 obtain a total resistance of about ~ 14.5 ohms.

446 All the HRM probes were inserted into a horizontal plane above the soil surface at breast
447 height. The heater and thermocouples were placed in a vertical position and the symmetry
448 was aligned (Fig. A1a). The distal part of each sensor was enclosed in a box (FEMATEL
449 100x100x55 mm) (Fig. A1b). The HRM probes were placed on the west side of the trunk
450 to avoid the maximum global solar radiation from the east side due to the Plant
451 Experimental Unit's features. All the equipment was wrapped with reflective insulation
452 to protect it from solar radiation (NOMAREFLEX) (Fig. A2a).



453

454 Figure A1. (a) Vertically and symmetry position of heater and thermocouples. Heater was
455 represented in black colour. Thermocouples were represented in red and blue colour, and
456 they were located at 0.6 cm upstream and downstream of the heater. (b) Protecting box
457 with the distal part of each sensor, resistances, and connectors.



458

459 Figure A2. (a) All heat ratio method probes equipment were wrapped with a reflective
460 insulation to protect it from solar radiation. (b) Exemplification of needle deep in a cross-
461 section trunk.



462 **Appendix B. List of the materials to construct and install the heat ratio method**
463 **probes**

- 464 - Thermocouple Extension. (EXPP-E-20-1000 T/C).
- 465 - Heater Extension. H05V-F. Two-wire cable. 5 mm².
- 466 - Adapter USB/RS232 (Digitus).
- 467 - Relay (Relay SSR Crydom DRA1-CMX60D10).
- 468 - Glacier Flex (500 FR).
- 469 - Anticondensation adhesive tape.
- 470 - Aluminium repair tape. 10 m x 50 mm. Argent.
- 471 - Gel accumulator (SET 2 ACUM 400GR N1).
- 472 - Sub-mini w/window purple (SMPW-E-M).
- 473 - Heat-shrink tube. Thermocouple: 6.4/3.2 mm, 3.2/1.5 mm and 2.4/1.5 mm.
- 474 - Heater: 6.0/3.0 mm

475 **Appendix C. Experimental setup**

476 The three pines were placed inside a module (6.4x16x4.5 m, width x length x height).
477 The module structure was made of hot-dip galvanised steel. A system of aluminium
478 profiles was placed on exterior walls. The roof was made of industrial-quality glass (4-2
479 mm). The front and sides glasses were double-glazed (4-2 mm), and the interior glasses
480 were single-glazed (4-2 mm). The extractor and fog system controlled the laboratory
481 conditions. Extractors were a monoblock of galvanised steel, with reversible flat or
482 curved blade propellers, automatic blind, polypropylene front protection, motor: IP-55
483 protection, tension III/230/440 V-50 HZ. The fog system worked at high pressure (60
484 kg/cm²). The system contained special high-pressure misting nozzles and an HP FFL
485 high-pressure nose with a non-drip valve to ensure that 90 % of droplets would be less
486 than 10 microns in size. The fog system was close to pine number 2 and at the same
487 distance from pine numbers 1 and 3. Pines were arranged in a straight line at the start of
488 the module. Pine number 1 was 1.5 m from pine number 2, and 3 m from pine number 3.
489 The global solar radiation recorder and the air humidity and temperature recorder were 2
490 m in a straight line from pine number 2. Pines were ~3 m high.

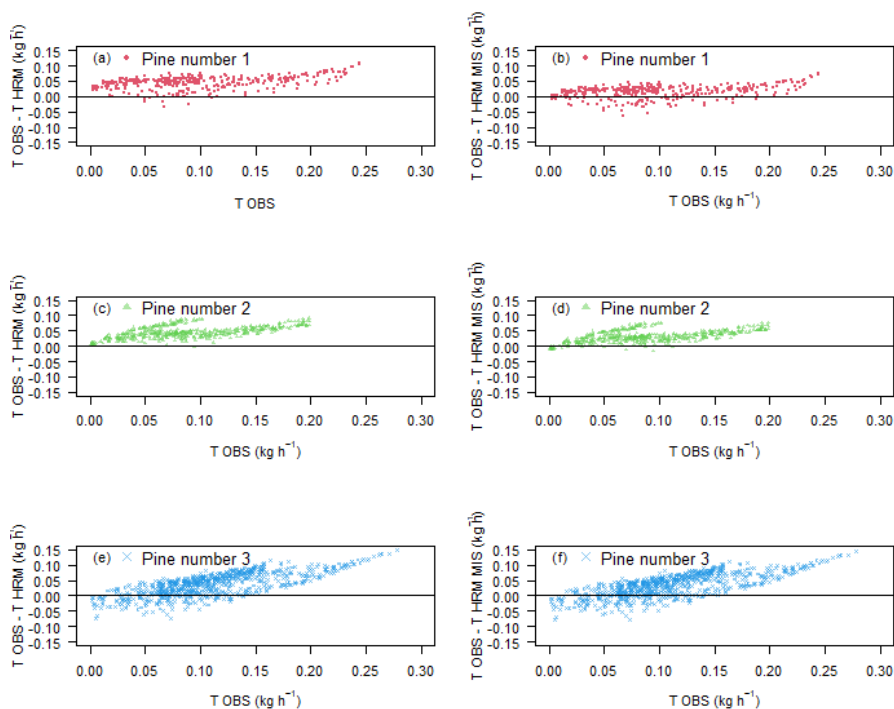
491

492

493



494 **Appendix D. Supplementary results**



495

496 Figure D1. (a), (c) and (e) Relationship between the transpiration difference between
497 methods: load cells and heat ratio method probes ($T_{OBS} - T_{HRM}$) vs. T_{OBS} . (b), (d), and (f)
498 Relationship between the transpiration difference between methods: load cells and heat
499 ratio method probes applying the probe misalignment correction proposed by Larsen et
500 al. (2020) ($T_{OBS} - T_{HRM MIS}$) vs. T_{OBS} .

501

502

503

504

505

506



507 Table D1. Mean and standard deviation of temperature probes distance respect the heater
508 probe and the corresponding root mean square. The correct distance between the
509 temperature and heater probes was 0.6 cm. The closest distance values to 0.6 cm indicate
510 the higher precision in probes insertion, therefore a minor correction in transpiration rates
511 values.

| | Pine number 1 | Pine number 2 | Pine number 3 |
|--|---------------|---------------|---------------|
| X ₁ (cm) | 0.69 ± 0.02 | 0.65 ± 0.01 | 0.62 ± 0.01 |
| X ₂ (cm) | -0.49 ± 0.02 | -0.55 ± 0.01 | -0.58 ± 0.01 |
| Root mean square of the distance to value | 0.078 | 0.050 | 0.020 |

512

513 **Code availability**

514 The code that supports the findings of this study are available from the corresponding
515 author upon reasonable request (sabaterblasco@gmail.com).

516 **Data availability**

517 The data that support the findings of this study are available from the corresponding
518 author upon reasonable request (sabaterblasco@gmail.com).

519 **Author contribution**

520 AV and JB conceptualised the study. AMS made the sensors under the supervision of
521 JAV and JB. AMS implemented the sensors and was responsible for the data processing
522 and the laboratory work. JAV wrote the script for the datalogger and was responsible for
523 the technical aspect of the study. AMS, AV and JAV worked on the data analysis. AMS
524 and JAV prepared the paper with inputs from all the co-authors. All authors worked in
525 the preparation and revision of the published work.

526 **Competing interests**

527 The authors declare that they have no conflict of interests.

528 **Acknowledgements**

529 We thank E. Riquelme for assistance in the laboratory work. We thank A. del Campo for
530 the transfer of knowledge about the heat ratio method probes building This study was
531 funded by the Spanish Ministry of Science, Innovation and Universities and the European
532 Regional Development Fund through research projects BLUEWATER-HYDROMED”



533 (PID2019-111332RB-C21 MICINN/FEDER), “INERTIA_HYDROMED” (PID2019-
534 111332RB-C22 MICINN/FEDER) and “VERSUS” (CGL2015-67466-R
535 MICINN/FEDER)”; and “IMAGINA– PROMETEOII/2019/110” funded by the
536 Generalitat Valenciana. A.M. Sabater was supported by a European Social Fund and the
537 Generalitat Valenciana with a PhD contract (ACIF/2018/279). The CEAM Foundation is
538 supported by the Generalitat Valenciana (Spain).

539 **References**

540 Allen, C.D. Breshears, D.D. McDowell, N.G.: On underestimation of global vulnerability
541 to tree mortality and forest die-off from hotter drought in the Anthropocene, *Ecosphere*.
542 6, 1–55, <https://doi.org/10.1890/ES15-00203.1>, 2015.

543

544 Allen, R. G., Pereira, L. S., Raes, D., Smith, M.: Crop evapotranspiration-Guidelines for
545 computing crop water requirements-FAO Irrigation and drainage paper 56, Fao,
546 Rome, 300(9), D05109, 1998.

547

548 Alvarado-Barrientos, M. S., Hernández-Santana, V., Asbjornsen, H.: Variability of the
549 radial profile of sap velocity in *Pinus patula* from contrasting stands within the seasonal
550 cloud forest zone of Veracruz, Mexico, *Agric. For. Meteorol.*, 168, 108-119,
551 <https://doi.org/10.1016/j.agrformet.2012.08.004>, 2013.

552

553 Bleby, T. M., Burgess, S. S., Adams, M. A.: A validation, comparison and error analysis
554 of two heat-pulse methods for measuring sap flow in *Eucalyptus marginata*
555 saplings, *Funct. Plant Biol.*, 31(6), 645-658, <https://doi.org/10.1071/FP04013>, 2004.

556

557 Burgess, S. S., Adams, M. A., Turner, N. C., Beverly, C. R., Ong, C. K., Khan, A. A.,
558 Bleby, T. M.: An improved heat pulse method to measure low and reverse rates of sap
559 flow in woody plants, *Tree physiol*, 21(9), 589-598.
560 <https://doi.org/10.1093/treephys/21.9.589>, 2001.

561

562 Burgess, S. S., Dawson, T. E.: Using branch and basal trunk sap flow measurements to
563 estimate whole-plant water capacitance: a caution, *Plant Soil*, 305(1), 5-13, [https://doi:
564 10.1007/s11104-007-9378-2](https://doi.org/10.1007/s11104-007-9378-2), 2008



565 Chirino, E., Bellot, J., Sánchez, J. R.: Daily sap flow rate as an indicator of drought
566 avoidance mechanisms in five Mediterranean perennial species in semi-arid southeastern
567 Spain. *Trees*, 25(4), 593-606, [https:// doi:10.1007/s00468-010-0536-4](https://doi.org/10.1007/s00468-010-0536-4), 2011.

568

569 Chirino Miranda, E., Heredia-Osorio, M., Granados, M. E., Vilagrosa, A., Manrique-
570 Alba, À., Ruiz-Yanetti, S., Andarcio, C., Bellot Abad, J. F.: Balance hídrico del suelo en
571 pinares con diferente densidad de arbolado, Efectos sobre el establecimiento de brinzales
572 de especies rebrotadoras bajo el dosel, *Cuadernos de la Sociedad Española de Ciencias*
573 *Forestales*, (41), 291-304, 2015.

574

575 Davis, T. W., Kuo, C. M., Liang, X., Yu, P. S.: Sap flow sensors: construction, quality
576 control and comparison, *Sensors*, 12(1), 954-971, <https://doi.org/10.3390/s120100954>,
577 2012.

578

579 del Campo, A. D., Fernandes, T. J., Molina, A. J.: Hydrology-oriented (adaptive)
580 silviculture in a semiarid pine plantation: How much can be modified the water cycle
581 through forest management?, *European J. Forest. Res.*, 133(5), 879-
582 894, <https://doi.org/10.1007/s10342-014-0805-7>, 2014.

583

584 Dix, M. J., Aubrey, D. P.: Recalibrating best practices, challenges, and limitations of
585 estimating tree transpiration via sap flow, *Curr. Forestry Rep.*, 7(1), 31-37,
586 <https://doi.org/10.1007/s40725-021-00134-x>. 2021.

587

588 Eliades, M., Bruggeman, A., Djuma, H., Lubczynski, M. W.: Tree water dynamics in a
589 semi-arid, *Pinus brutia forest*, *Water*, 10(8), 1039, <https://doi.org/10.3390/w10081039>,
590 2018.

591

592 Good, S. P., Noone, D., Bowen, G.: Hydrologic connectivity constrains partitioning of
593 global terrestrial water fluxes, *Science*, 349(6244), 175-177, [https:// doi.org/
594 10.1126/science.aaa5931](https://doi.org/10.1126/science.aaa5931), 2015.

595



- 596 Granier, A.: Evaluation of transpiration in a Douglas-fir stand by means of sap flow
597 measurements. *Tree physiol*, 3(4), 309-320, <https://doi.org/10.1093/treephys/3.4.309>,
598 1987.
599
- 600 Grossiord, C., Buckley, T. N., Cernusak, L. A., Novick, K. A., Poulter, B., Siegwolf, R.
601 T., Sperry, J.S., McDowell, N. G.: Plant responses to rising vapor pressure deficit, *New*
602 *Phytol.*, 226(6), 1550-1566, <https://doi.org/10.1111/nph.16485>, 2020.
603
- 604 Fernandes, T. J., Campo, A. D. D., Garcia-Bartual, R., Gonzalez-Sanchis, M.: Coupling
605 daily transpiration modelling with forest management in a semiarid pine
606 plantation, *iForest-Biogeosc. For.*, 9(1), 38, <https://doi.org/10.3832/ifor1290-008>, 2015.
607
- 608 Fernández, J. E., Palomo, M. J., Diaz-Espejo, A., Clothier, B. E., Green, S. R., Girón, I.
609 F., Moreno, F.: Heat-pulse measurements of sap flow in olives for automating irrigation:
610 tests, root flow and diagnostics of water stress, *Agric. Water Manage.*, 51(2), 99-123,
611 [https://doi.org/10.1016/S0378-3774\(01\)00119-6](https://doi.org/10.1016/S0378-3774(01)00119-6), 2001.
612
- 613 Forster, M. A.: How reliable are heat pulse velocity methods for estimating tree
614 transpiration?, *Forests*, 8(9), 350, <https://doi.org/10.3390/f8090350>, 2017
615
- 616 Fuchs, S., Leuschner, C., Link, R., Coners, H., Schuldt, B.: Calibration and comparison
617 of thermal dissipation, heat ratio and heat field deformation sap flow probes for diffuse-
618 porous trees, *Agric. For Meteorol.*, 244, 151-161.
619 <https://doi.org/10.1016/j.agrformet.2017.04.003>, 2017.
620
- 621 Hartmann, H., Schuld, B., Sanders, T.G., Macinnis-Ng, C., Boehmer, H.J., Allen, C.D.,
622 Bolte, A., Crowther, T.W., Hansen, M.C., Medlyn, B.E., RUEHR, N.K., Anderegg, R.R.L.:
623 Monitoring global tree mortality patterns and trends, Report from the VW symposium
624 'Crossing scales and disciplines to identify global trends of tree mortality as indicators of
625 forest health', *New Phytol*, 217(3) 984–987, <http://doi.wiley.com/10.1111/nph.14988>,
626 2018.
627



- 628 Hatton, T. J., Greenslade, D., Dawes, W. R.: Integration of sapflow velocity in elliptical
629 stems, *Tree physiol.*, 11(2), 185-196, <https://doi.org/10.1093/treephys/11.2.185>, 1992.
630
- 631 Huber, B.: Weitere quantitative Untersuchungen über das Wasserleitungssystem der
632 Pflanzen. *Fahrbücher für Wissenschaftliche Botanik*, 67, 877-959, 1928.
633
- 634 IPCC, Masson-Delmotte, V., Zhai, P., Pirani A., Connors, S.L., Péan, C., Berger S., Caud, N.,
635 Chen, Y., Goldfarb, L., Gomis, M.I., Huang, M., Leitzell, K., Lonnoy, E., Matthews, J.B.R.,
636 Maycock, T.K., Waterfield, T., Yelekçi, O., Yu, R., Zhou, B.: *Climate Change 2021: The Physical
637 Science Basis. Contribution of Working Group I to the Sixth Assessment Report of the
638 Intergovernmental Panel on Climate Change*, Cambridge University Press, 2021.
639
- 640 Jasechko, S., Sharp, ZD., Gibson, J.J., Birks, S.J., Yi, Y., Fawcett, P.J.: Terrestrial water
641 fluxes dominated by transpiration. *Nature*, 496, 347-350,
642 <https://doi.org/10.1038/nature11983>, 2013.
643
- 644 Larsen, E. K.: *Transpiration patterns of Pinus halepensis Mill. in response to
645 environmental stresses in a Mediterranean climate. Doctoral dissertation, University of
646 Alicante*, 2021.
647
- 648 Larsen, E. K., Palau, J. L., Valiente, J. A., Chirino, E., Bellot, J.: Long-term probe
649 misalignment and proposed quality control using the heat pulse method for transpiration
650 estimations, *Hydrol. Earth Syst. Sci.*, 24(5), 2755-2767, [https://doi.org/10.5194/hess-24-
651 2755-2020](https://doi.org/10.5194/hess-24-2755-2020), 2020.
652
- 653 Lefcheck, Jonathan S.: piecewiseSEM: Piecewise structural equation modelling in R for
654 ecology, evolution, and systematics. *Methods Ecol. Evol.*, 7(5): 573-579, [https://doi.org/
655 10.1111/2041-210X.12512](https://doi.org/10.1111/2041-210X.12512), 2016.
656
- 657 Lindner, M., Maroschek, M., Netherer, S., Kremer, A., Barbati, A., Garcia-Gonzalo, J.,
658 Seidl, R., Delzon, S., Corona, P., Kolström M., Lexer, M., Marchetti, M.: Climate change
659 impacts, adaptive capacity, and vulnerability of European forest ecosystems, *Forest Ecol.
660 Manag.*, 259(4) 698-709, <https://doi.org/10.1016/j.foreco.2009.09.023>, 2010.



- 661 Lionello, P., Scarascia, L.: The relation between climate change in the Mediterranean
662 region and global warming, *Reg. Environ. Change*, 18(5), 1481-1493,
663 <https://doi.org/10.1007/s10113-018-1290-1>, 2018.
- 664
- 665 López-Bernal, Á., Alcántara, E., Villalobos, F. J.: Thermal properties of sapwood of fruit
666 trees as affected by anatomy and water potential: errors in sap flux density measurements
667 based on heat pulse methods, *Trees*. 28(6), 1623-1634, [https://doi.org/10.1007/s00468-](https://doi.org/10.1007/s00468-014-1071-5)
668 014-1071-5, 2014.
- 669 Looker, N., Martin, J., Jencso, K., Hu, J.: Contribution of sapwood traits to uncertainty
670 in conifer sap flow as estimated with the heat-ratio method, *Agric.For. Meteorol.*, 223,
671 60-71, <https://doi.org/10.1016/j.agrformet.2016.03.014>, 2016.
- 672
- 673 Manrique-Alba, À.: Ecohydrological relationships in pine forests in water-scarce
674 environments, PhD thesis, University of Alicante, Alicante, Spain, 2017.
- 675
- 676 Marshall, D. C.: Measurement of sap flow in conifers by heat transport. *Plant*
677 *physiol.*, 33(6), 385, <https://doi.org/10.1104/pp.33.6.385>, 1958.
- 678
- 679 Nakagawa, S. Schielzeth, H.: A general and simple method for obtaining R² from
680 generalized linear mixed-effects models, *Methods Ecol. Evol.* 4(2), 133-142.
681 <https://doi.org/10.1111/j.2041-210x.2012.00261.x>, 2013.
- 682
- 683 Quézel, P.: Taxonomy and biogeography of Mediterranean pines (*Pinus*
684 *halepensis* and *P. brutia*), in: *Ecology, Biogeography and Management of Pinus*
685 *halepensis* and *P. brutia* forest ecosystems in the Mediterranean Basin, edited by:
686 Néeman, G., Trabaud, L., Backhuys Publishers, Leiden, pp. 1–12, 2000.
- 687
- 688 R Core Team.: R: A language and environment for statistical computing. R Foundation
689 for Statistical Computing, Vienna, Austria, 2021.
- 690
- 691 Rubilar, R. A., Hubbard, R. M., Yañez, M. A., Medina, A. M., Valenzuela, H. E.:
692 Quantifying differences in thermal dissipation probe calibrations for *Eucalyptus globulus*



- 693 species and *E. nitens* × *globulus* hybrid, *Trees*, 31(4), 1263-1270,
694 <https://doi.org/10.1007/s00468-017-1545-3>, 2017.
- 695
- 696 Ruiz-Yanetti, S., Chirino, E., Bellot, J.: Daily whole-seedling transpiration determined
697 by minilysimeters, allows the estimation of the water requirements of seedlings used for
698 dryland afforestation, *J. Arid. Environ.*, s, 124, 341-351,
699 <https://doi.org/10.1016/j.jaridenv.2015.08.017>, 2016.
- 700
- 701 Sabater, A. M., Vicente, E., Morcillo, L., Campo, A. D., Larsen, E. K., Moutahir, H.,
702 Pastor, F., Palau JL., Bellot, J., Vilagrosa A.: Water-Based Forest Management of
703 Mediterranean Pine Forests, in: *Pines and Their Mixed Forest Ecosystems in the*
704 *Mediterranean Basin*, edited by: Ne'eman, G., Osem, Y., Cham, pp. 727-746,
705 https://doi.org/10.1007/978-3-030-63625-8_34, 2021.
- 706 Scheidegger, Y., Saurer, M., Bahn, M., Siegwolf, R.: Linking stable oxygen and carbon
707 isotopes with stomatal conductance and photosynthetic capacity: a conceptual
708 model. *Oecologia*, 125(3), 350-357, <https://doi.org/10.1007/s004420000466>, 2000.
- 709
- 710 Smith, D. M., Allen, S. J.: Measurement of sap flow in plant stems, *J. Exp. Bot.*, 47(12),
711 1833-1844, <https://doi.org/10.1093/jxb/47.12.1833>, 1996.
- 712
- 713 Sperry, J. S., Venturas, M. D., Todd, H. N., Trugman, A. T., Anderegg, W. R., Wang, Y.,
714 Tai, X.: The impact of rising CO₂ and acclimation on the response of US forests to global
715 warming, *Proc. Natl. Acad. Sci.*, 116(51), 25734-25744, [https://doi.org/](https://doi.org/10.6084/m9.figshare.8805110)
716 [10.6084/m9.figshare.8805110](https://doi.org/10.6084/m9.figshare.8805110), 2019.
- 717
- 718 Steppe, K., De Pauw, D. J., Doody, T. M., Teskey, R. O.: A comparison of sap flux
719 density using thermal dissipation, heat pulse velocity and heat field deformation
720 methods, *Agric. For. Meteorol.*, 150(7-8), 1046-1056,
721 <https://doi.org/10.1016/j.agrformet.2010.04.004>, 2010.
- 722
- 723 Sun, H., Aubrey, D. P., Teskey, R. O.: A simple calibration improved the accuracy of the
724 thermal dissipation technique for sap flow measurements in juvenile trees of six
725 species, *Trees*, 26(2), 631-640, <https://doi.org/10.1007/s00468-011-0631-1>, 2012.



- 726 Swanson, R. H.: Numerical and experimental analyses of implanted-probe heat pulse
727 velocity theory. Ph.D. Thesis, University of Alberta, Edmonton, Canada, 298, 1983.
728
- 729 Swanson, R.H.: Significant historical developments in thermal methods for measuring
730 sap flow in trees, *Agric. For. Meteorol.*, 72, 113-132, [https://doi.org/10.1016/0168-](https://doi.org/10.1016/0168-1923(94)90094-9)
731 [1923\(94\)90094-9](https://doi.org/10.1016/0168-1923(94)90094-9), 1994.
- 732 Swanson, R. H., Whitfield, D. W. A.: A numerical analysis of heat pulse velocity theory
733 and practice, *J. Exp. Bot.*, 32(1), 221-239, 1981.
734
- 735 Vandegehuchte, M. W., Steppe, K.: Improving sap flux density measurements by
736 correctly determining thermal diffusivity, differentiating between bound and unbound
737 water, *Tree physiol.*, 32(7), 930-942, <https://doi.org/10.1093/jxb/32.1.221>, 2012.
- 738 Vergeynst, L.L., Vandegehuchte, M.W., McGuire, M.A., Teskey, R.O., Steppe, K.:
739 Changes in stem water content influence sap flux density measurements with thermal
740 dissipation probes, *Trees*, 28, 949–955, <https://doi.org/10.1007/s00468-014-0989-y>,
741 2014.
742
- 743 Vicente, E., Vilagrosa, A., Ruiz-Yanetti, S., Manrique-Alba, À., González-Sanchís, M.,
744 Moutahir, H., Chirino, E., del Campo, A., Bellot, J.: Water balance of Mediterranean
745 *Quercus ilex* L. and *Pinus halepensis* mill. forests in semiarid climates: A review in a
746 climate change context, *Forests*, 9(7), 426, <https://doi.org/10.3390/f9070426>, 2018.
747
- 748 Williams, D. G., Cable, W., Hultine, K., Hoedjes, J. C. B., Yopez, E. A., Simonneaux,
749 V., Er-Raki, S., Boulet, G., Bruin, H.A.R., Chehbouni, A., Timouk, F.:
750 Evapotranspiration components determined by stable isotope, sap flow and eddy
751 covariance techniques, *Agric. For. Meteorol.*, 125(3-4), 241-258,
752 <https://doi.org/10.1016/j.agrformet.2004.04.008>, 2004.
753
- 754 Wiedemann, A., Marañón-Jiménez, S., Rebmann, C., Herbst, M., Cuntz, M.: An
755 empirical study of the wound effect on sap flux density measured with thermal dissipation
756 probes, *Tree physiol.*, 36(12), 1471-1484, <https://doi.org/10.1093/treephys/tpw071>, 2016.



757 Zambrano-Bigiarini M.: hydroGOF: Goodness-of-fit functions for comparison of
758 simulated and observed hydrological time series R package version 0.4-0,
759 <https://doi.org/10.5281/zenodo.839854>, 2020.